Article

J. Mex. Chem. Soc. **2025**, *69*(3)
Regular Issue

ISSN-e 2594-0317

Triazoles Nanoencapsulation in Polylactic Acid to Reduce Phytotoxicity in Roots

Jahsive S. Quintero-Beltrán[1], Gabriela Sánchez-Viveros[1], Roberto G. Chiquito-Contreras[1], Greta H. Rosas-Saito[2], Randy Ortiz-Castro[2], Israel Bonilla-Landa[2], José L. Olivares-Romero[2], Felipe Barrera-Méndez[2,3*]

[1]Facultad de Ciencias Agrícolas, Universidad Veracruzana. Xalapa, Veracruz, México.
[2]Red de Estudios Moleculares Avanzados, Instituto de Ecología AC, Xalapa, Veracruz, México.
[3]Investigador por México-CONAHCYT. Xalapa, Veracruz, México.

***Corresponding author:** Felipe Barrera-Méndez, email: felipe.barrera@inecol.mx

Received April 19th, 2024; Accepted September 17th, 2024.

DOI: http://dx.doi.org/10.29356/jmcs.v69i3.2254

Abstract. The use of effective fungicides, such as propiconazole, a high-efficacy and broad-spectrum systemic fungicide, has been a common commercial strategy to combat fungal diseases. However, their indiscriminate and uncontrolled use provokes phytotoxicity in plant roots. Therefore, the objective of this study is to reduce the root phytotoxicity of triazole fungicides through their nanoencapsulation in biodegradable polylactic acid polymer matrices. Using the emulsion and solvent evaporation encapsulation method, the obtained nanoparticles had a hydrodynamic diameter of approximately 200 to 400 nm, an encapsulation efficiency of around 40 %, a smooth surface, and a zeta potential close to -40 mV, having great colloidal stability. Experiments with *Arabidopsis thaliana* demonstrated that the nanoencapsulation of a fungicide derived from propiconazole reduced its phytotoxicity, increasing the length of the roots over 70 % more than when the molecule was applied directly, losing only about 15 % of its antifungal activity, as shown by the test performed on *Fusarium solani*. This suggests that nanoencapsulation with biodegradable polymer matrices acts as a protective mechanism for plant roots, which may have practical applications in crop protection and the promotion of sustainable agriculture.
Keywords: Fungicide; fusarium; phytotoxicity; propiconazole; polylactide.

Resumen. El uso de fungicidas eficaces, como el propiconazol, un fungicida sistémico de alta eficacia y amplio espectro, ha sido una estrategia comercial común para combatir las enfermedades fúngicas. Sin embargo, su uso indiscriminado y descontrolado provoca fitotoxicidad en las raíces de las plantas. Por lo tanto, el objetivo de este estudio es reducir la fitotoxicidad radicular de fungicidas triazoles mediante su nanoencapsulación en matrices poliméricas de ácido poliláctico biodegradables. Utilizando el método de encapsulación por emulsión y evaporación de solvente, las nanopartículas obtenidas tuvieron un diámetro hidrodinámico de aproximadamente 200 a 400 nm, una eficiencia de encapsulación de alrededor del 40 %, una superficie lisa y un potencial zeta cercano a -40 mV, teniendo una gran estabilidad coloidal. Experimentos con *Arabidopsis thaliana* demostraron que la nanoencapsulación de un fungicida derivado del propiconazol redujo su fitotoxicidad, aumentando la longitud de las raíces un 70 % más que cuando la molécula se aplicó directamente, perdiendo sólo alrededor del 15 % de su actividad antifúngica, como lo demuestra la prueba realizada en *Fusarium solani*. Esto sugiere que la nanoencapsulación con matrices poliméricas biodegradables actúa como un mecanismo protector para las raíces de las plantas, lo que puede tener aplicaciones prácticas en la protección de cultivos y la promoción de la agricultura sostenible.
Palabras clave: Fungicida, fusarium; fitotoxicidad; propiconazol; polylactida.

J. Mex. Chem. Soc. **2025**, *69*(3)
Regular Issue

ISSN-e 2594-0317

Introduction

As recent research has demonstrated, fungal diseases pose a significant challenge to global agriculture and food security. Phytopathogenic fungi often cause some of the most devastating impacts in both natural ecosystems and agricultural production systems, leading to agricultural epidemics. [1] These fungal diseases have been confirmed as one of the primary reasons behind the annual reduction in global food production, ranging from 10 % to 40 %. [2] Given that economically valuable tree groups, such as avocado, are among the most affected, it is important to create effective and controlled solutions.

Consequently, prevention and treatment strategies have been implemented to mitigate the negative impacts generated by this pathogenic agent, using effective fungicides. One such example is the use of propiconazole, a systemic fungicide belonging to the triazole family. It is widely used worldwide as a phytosanitary agent to combat fungal diseases and is known for its broad-spectrum antifungal action. [3] However, its excessive and indiscriminate use can lead to phytotoxic effects on plant roots. [4] Therefore, research efforts have been undertaken to improve its formulation and chemical composition to minimize its environmental impact. Previous works synthesized and evaluated a series of propiconazole analogs incorporating the 1,2,4-triazole heterocycle, which is the pharmacophore conferring fungicidal effects to the molecules. The inhibitory activity of this competent compound is also enhanced by modifying its chemical composition, with the addition of halogens to fungicidal products altering significant elements in the molecule, providing greater biological efficacy and specificity. [5] Thus, the substitution of hydrogen atoms with fluorinated groups enhances the lipophilic affinity of the molecule, enabling greater accumulation at active enzyme sites. [6]

The scientific community has been engaged in seeking novel and cost-effective approaches as alternatives to conventional fungicides. In this context, the incorporation of nanoscience has the potential to effectively counteract the unfavorable aspects of traditional agrochemicals. [7] Nanotechnology promotes the creation of components with less harmful biomaterials and ingredients, greater durability of active components, a positive biological safety profile, and increased effectiveness against specific pests. [8,9] To mitigate the phytotoxicity on roots associated with the application of propiconazole, the use of nanoencapsulation with polylactic acid (PLA) as wall material is suggested as an economically feasible and environmentally friendly option for disease management. Previous research in this field has supported nanoencapsulation as an effective approach for reducing phytotoxicity. For instance, Shalini et al. reported experiments in cytotoxicity where encapsulation with sodium alginate resulted in a minimal reduction proportional to the concentration used in nanoparticles. [10] Likewise, other studies related to fungicides and herbicides have sought to mitigate their environmental impact through techniques such as coating with laminar kaolinite, nanoparticles of nanoscale rice, and amino-activated iron oxide (II,III) nanoparticles. [11-13] Another example was with the herbicides imazapir and imazapic, loaded within chitosan nanoparticles against the weed *Bidens pilosa*, where their toxicity was reduced in assays and cell cultures compared to their free formulation. [14] The objective of this study is to reduce the phytotoxicity of triazole fungicides by encapsulating them in PLA nanospheres while maintaining their antifungal activity.

Experimental

Reagents

Sodium Citrate, N-Bromosuccinimide - B81255-5G, p-toluensulfonic acid monohydrate - 402885, Potassium carbonate - 209619, 1,2,4-triazole - T46108, Phenyl Magnesium Bromide – 331376. All the chemical reagents were obtained from Sigma-Aldrich. Hexane and Dichloromethane were from Pochteca. Propiconazole was obtained from Prozan® commercial fungicide. Each of these compounds underwent a purification process before being used. Industrial-grade polylactic acid was obtained from Makerbot filament for 3D printing.

Biological material

A strain of *Fusarium solani* was chosen for antifungal tests, as it is a species that attacks commercially significant crops. Cultures of five *F. solani* isolates provided by the Molecular Biology Laboratory of the

J. Mex. Chem. Soc. **2025**, *69*(3)
Regular Issue

ISSN-e 2594-0317

BioMimic Scientific and Technological Cluster were grown on potato dextrose agar (PDA) and incubated for one week at 27 ± 1 °C with periodic subculturing.

Arabidopsis thaliana seeds were provided by the Environmental Microbiology Laboratory of the BioMimic Scientific and Technological Cluster.

Purification of commercial propiconazole (PPZ)

Pure propiconazole was obtained from the Prosan® commercial formulation using open column chromatography. Silica gel with a particle size of 40-63 μm was used as the stationary phase, while a mixture composed of dichloromethane and isopropanol in a ratio of 98:2 was used as the mobile phase. The thin-layer chromatography technique, using phosphomolybdic acid as a revealing agent, was applied to determine fractions containing propiconazole without impurities.

Synthesis route

Bonilla et al. developed a synthetic route for the preparation of propiconazole-derived compounds, which was executed for this experimentation. [5] The molecules described in the article were used following their procedures, selecting the one that showed the highest percentage of inhibition against the *Fusarium* fungus, which turned out to be molecule 1-Phenyl-2-(1H-1,2,4-triazol-1-yl)-1-[4-(trifluoromethyl)phenyl]propan-1-ol, along with the one that exhibited the lowest toxicity in plants, which was molecule 2-(1H-1,2,4-Triazol-1-yl)-1-[4-(trifluoromethyl)phenyl]propan-1-one (molecules 6 and 4 in scheme 1, respectively).

Molecules 4 and 6 were synthesized starting from ketones 1 and 2, which were reacted with NBS in acetonitrile under reflux to yield the products 3 and 4. A SN2 reaction on the previous products with 1,2,4-triazole afforded the first target 4 in 80 % yield and the intermediate 5, which upon treatment with phenyl magnesium bromide in THF generated second the target product 6. It is worth noting that the yields were very similar to those already reported.

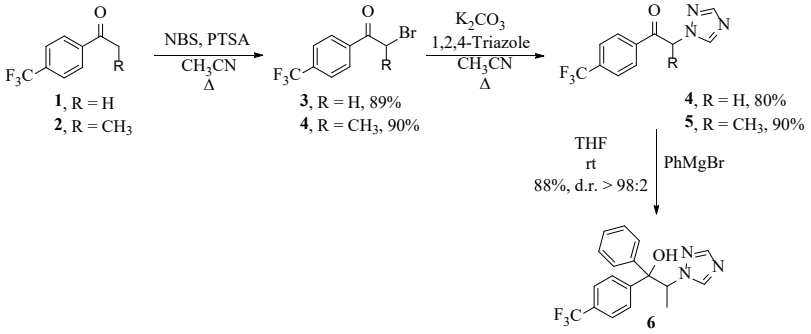

Scheme 1. Synthesis route for propiconazole derivatives.

Preparation of Nanoparticles (NPs)

The emulsification and solvent evaporation method was used for the preparation of nanoparticles (NPs) loaded with an active ingredient (AI), either PPZ or one of its derivatives: tertiary alcohol (TA), or ketone (KE), as well as NPs without load used as control Barrera-Méndez 2019). [15,16] This was accomplished by dissolving 10 mg of the respective AI in 5 mL of an organic solution of PLA in dichloromethane (DCM), with a concentration of 5 mg of PLA per mL of DCM. Subsequently, the organic phase was added to 15 mL of an aqueous solution of 1 mM sodium citrate (used as emulsifier). The mixture was sonicated using a Sonics Vibra Cell ultrasonic processor at a frequency of 20 kHz with 70 % amplitude for three 10 second intervals, placed in an ice bath for cooling between each interval. The organic fraction of the emulsion was evaporated using a Büchi R-100 rotary evaporator at a temperature of 40 °C at 38.1 kPa. Three washes with Milli-Q water were then performed to remove any free AI. The resulting suspension was distributed into microcentrifuge tubes and centrifuged at 5000 x g for 30 minutes. Finally, the NPs were concentrated in a stabilizing solution of 0.1 mM sodium citrate.

J. Mex. Chem. Soc. **2025**, *69*(3)
Regular Issue

ISSN-e 2594-0317

NP characterization

The hydrodynamic size, zeta potential (ξ), and polydispersity index (PDI) were determined using the dynamic light scattering (DLS) technique with a Nano-ZS90 Zetasizer from Malvern Instruments.

The encapsulation efficiency (EE) was calculated using Eq.1:

$$EE = \frac{P_R}{P_0} * 100 \quad (1)$$

where P_0 is the AI mass of the compound used in the encapsulation process and P_R is the AI mass released in ethanol. To quantify the amount of propiconazole contained in the nano-spheres, it was necessary for them to release their load into an ethanol release medium. Initially, the NPs were sedimented by centrifuging for 30 minutes at 5000 x g, and then removing the water and citrate. After that, 1 mL of ethanol was added and put in a Cole-Parmer Model 08895-43 ultrasonic bath for 30 minutes to "break" the NPs. The suspension with NPs was then centrifuged at 15 000 x g for 30 minutes, and the supernatant was removed. The concentration of AI in the ethanol was measured with a Thermo Scientific Genesys 10S UV-Vis spectrophotometer, using a wave length of 258 nm for the TA derivative, 282 nm for KE, and 270 nm for purified PPZ. Data was processed using SigmaPlot and The R Project software.

Finally, SEM images were obtained using a FEI Quanta FEG 250 field emission scanning electron microscope to observe the morphology of the NPs.

Antifungal activity essay

Following the methodology of Barrera-Méndez et al., *in vitro* antifungal activities of NPs were determined. [16] 4 µL of a conidial suspension of *F. solani* were introduced into the center of each well of a 12 well cell culture plate containing 1 mL of solid potato-dextrose-agar (PDA) medium enriched with 100 µM of AI of the respective treatments. Plates were incubated at a temperature of 28 °C ± 1 °C without light for 5 days. Three controls were used: the growth control, inoculating the spores in solid PDA without any treatment; one control with 5 % ethanol to demonstrate that the ethanol used for diluting the non-encapsulated AI has low antifungal activity; and one control with PLA nanospheres, but without any fungicide, to evaluate if the wall material has any antifungal activity. The experiment had 5 repetitions. The growth control can be used as negative control, since it only has the spores without any treatment. The treatment of propiconazole in its free form (F-PPZ) can be used as a positive control, since it is a molecule widely used as fungicide to control *F. solani* infections. Table 1 shows the code for each treatment tested.

Table 1. Code and conditions for the different treatments tested.

Name	Fungicide	Condition	Components
PLA	None (Control)	Nanospheres	Polylactic acid
etOH	None (Control)	Free form	Ethanol
N-PPZ	Propiconazole	Nanoencapsulated	Propiconazole + Polylactic acid
F-PPZ	Propiconazole	Free form (Positive control)	Propiconazole + Ethanol
N-TA	Tertiary alcohol	Nanoencapsulated	Tertiary alcohol + Polylactic acid
F-TA	Tertiary alcohol	Free form	Tertiary alcohol + Ethanol
N-KE	Ketone	Nanoencapsulated	Ketone + Polylactic acid
F-KE	Ketone	Free form	Ketone + Ethanol
C-	None (Control)	Growth control (Negative control)	None

J. Mex. Chem. Soc. **2025**, *69*(3)
Regular Issue

ISSN-e 2594-0317

Release profile

Each treatment was dispersed in 1 mL of an aqueous medium with 5% ethanol and pH 6 to simulate the conditions of the PDA used in the antifungal activity experiments, and then introduced in cellulose tubes of 12-14 kD. Each tube was then placed in 99 mL of the same aqueous medium. This was done in an amber glass flask kept under constant agitation at 200 rpm at a temperature of approximately 28 °C. The experiment was conducted in triplicate, and the initial AI concentration within the membrane was 1 mg/mL in all experiments. At specified time intervals, a sample was withdrawn and replaced with an equal amount of release medium. The concentration of the samples was measured using UV-visible spectrophotometry at 270 nm for propiconazole and 258 nm for the derivative. The amount of propiconazole subjected to dialysis and the size of the release medium were determined to achieve a final concentration of 0.01 mg/mL, significantly below the previously reported solubility of PPZ in water at 25 °C (0.1 mg/mL).

Phytotoxicity test

Arabidopsis thaliana seeds were pre-washed with 96 % ethanol before the experiment. They were shaken in a thermoshaker for 30 seconds and centrifuged for 7 minutes at 1200 rpm. Ethanol was removed, and the seeds were washed with a 20 % chlorine solution, shaken again, and centrifuged under the same conditions. They were rinsed with sterile distilled water and the agitation and centrifugation process was repeated six times. In the seventh wash, the seeds were placed in 1 mL of water in a microcentrifuge tube and refrigerated at 4 °C for 48 hours. Phytotoxicity was evaluated for NPs loaded with PPZ, TA, and KE in both nanoencapsulated and free forms using the following procedure: Murashige and Skoog medium (0.2x Sigma Aldrich, Cat. M5524) was used for the germination of previously disinfected seeds and supplemented with the treatments. 8 seeds were placed on each Petri dish. Finally, Petri dishes were placed in a plant growth chamber with conditions of 16 hours of light followed by 8 hours of darkness, at a constant temperature of 22 °C and a relative humidity of 80 %. Evaluation and photographs were taken at 10 days after germination. Measurements were taken of the main root length, and number of lateral roots. The counting of lateral roots was done by identifying those attached to the main root. The lateral root density was calculated by dividing the number of lateral roots by the length of the main root, expressed as NRL/cm. Descriptive statistical analyses were performed, and a significant difference in phytotoxicity tests was analyzed using R Studio software. The experiment had 6 repetitions.

Results and discussion

Characterization of NPs

The hydrodynamic size, zeta potential, and polydispersity of NPs loaded with PPZ, TA, and KE are presented in Table 2. NPs synthesized using the emulsification and solvent evaporation technique exhibit a homogeneous size distribution. The PDI is lower for the NPs of the derivatives, resulting in more uniform sizes. In all treatments, the NPs exhibit a zeta potential near -40 mV, preventing aggregation of the particles by repelling each other and promoting their stability in an aqueous solution.

Table 2. Characterization of nanoparticles obtained through the solvent emulsion and evaporation method.

NPs	Zeta Potential (mV)	Hydrodynamic Diameter (nm)	Polydispersity Index	Encapsulation Efficiency (%)
PLA	-29.40 ± 3.14	478.2 ± 77.13	0.232 ± 0.06	N/A
N-PPZ	-39.26 ± 7.81	353.05 ± 38.13	0.183 ± 0.18	41.13 ± 2.79
N-TA	-41.46 ± 6.62	380.29 ± 33.09	0.145 ± 0.09	42.05 ± 4.8
N-KE	-39.08 ± 4.45	234.29 ± 52.86	0.129 ± 0.12	27.53 ± 7.29

J. Mex. Chem. Soc. **2025**, *69*(3)
Regular Issue

ISSN-e 2594-0317

Fig. 1 display images captured by the scanning electron microscope. The images depict nanoparticles with a spherical shape and exhibit a size distribution composed of two groups for those loaded with PPZ and KE, consistent with the data obtained from the hydrodynamic diameter and PDI.

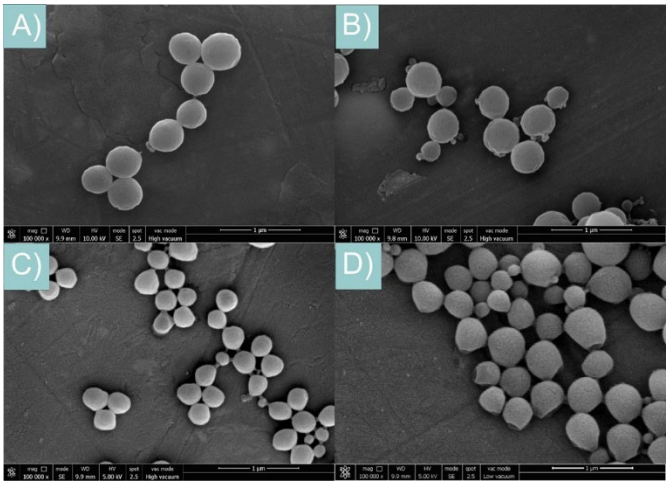

Fig. 1. SEM Images for the different nanoencapsulated treatments. **(A)** N-TA, **(B)** N-PPZ, **(C)** N-KE, **(D)** PLA.

In Fig. 1 **(D)**, it is evident that when an AI is not present, the nanoparticles tend to lose their spherical form. Nevertheless, the PLA NPs originally are spherical, but the electron beam modifies their form when the image is acquired as it burns the polymer. This effect was not present when the NPs are loaded. The PLA NPs had sizes ranging from approximately 400 to 500 nm, with a zeta potential of -29.4 mV and a PDI of 0.259, demonstrating a greater size distribution variation among the NPs. [17] The larger size of the PLA nanospheres can be explained as follows: when washing the nanospheres to remove the non-encapsulated fungicide and excess of emulsifier, the treatments go through a centrifugation process that precipitates these nanoparticles. During said centrifugation, the particles become more compacted at the bottom of the tube, forming a pellet that cannot be resuspended. This generates a reduction in particle size, since the largest particles are also the heaviest. As the PLA nanospheres do not contain fungicide, they could be lighter and, when the particles from this treatment were washed, they did not form the aforementioned pellet, thus preserving their larger particles in suspension. Having maintained both their smaller and lager particles, this also explains the higher polydispersity obtained. Nanoparticles with dimensions ranging from 300 to 400 nanometers are suitable for serving as delivery carriers. [18] The formulations exhibit a high zeta potential, providing them with great stability in aqueous dispersion. The data obtained during the characterization of N-PPZ aligns with similar studies on nanoencapsulated fungicides, where nanoparticles with an average size of 370 nm and a zeta potential exceeding -30 mV have been observed. [19] Meanwhile, Banpean et al. reported nanoparticles with PLA of 320 nm. [20] Following the categorization of active ingredient delivery systems using nanoparticles, the obtained nanoparticles loaded with PPZ or its derivatives can be classified within the category of biopolymer-coated nanosphere, where PLA acts as the membrane surrounding the active ingredient. [21] The hydrodynamic size and morphology of the empty spheres is consistent with previous observations and electron micrographs that have documented a range of 400 to 700 nm. [22-24] Meanwhile, authors like Wei et al. observe NPs with PLA in sizes ranging from 493 to 669 nm, displaying similar morphologies to those containing PPZ, as evidenced by the presence of biopolymer remnants in scanning electron microscopy. [25]

Zeta potential is an indicator that reflects the surface charge of particles and is influenced by changes in the interface with the dispersing medium. A zeta potential value within the range of ± 30 mV is considered crucial for maintaining the physicochemical stability of a colloidal suspension. This is because the presence of significant repulsive forces prevents particle aggregation through occasional collisions with surrounding

J. Mex. Chem. Soc. **2025**, *69*(3)
Regular Issue

ISSN-e 2594-0317

nanoparticles. Consequently, we can state that nanoparticles exhibit a considerably high or favorable zeta potential for their stability. [26,27]

It is important to note that colloidal suspensions typically do not exhibit phase separation until several months after their preparation, which is further diminished by Brownian motion. [28,29] To ensure stability, we have investigated key factors influencing it, such as NP size, zeta potential, drug content, and release. Our results support the significance of these parameters.

Antifungal activity essay

Fig. 2 shows a representative image of the 12 well plates containing the different treatments tested. The control groups display profuse cottony mycelial formation without visible pigmentation. The F-TA and F-KE treatments exhibited a yellow coloration, with reduced mycelial growth. On the other hand, the N-TA and N-KE treatments showed a smaller growth area, displaying brown coloration within the mycelium, and an asymmetric configuration, suggesting stress in the fungus's development and the appearance of a surrounding cottony edge. [1]

A reddish and brownish discoloration characteristic of fungal organism stress was detected. The structure of the fungal cell wall is complex and plays a vital role in shaping fungal growth. Furthermore, this cell wall has the ability to protect fungal cells from environmental stress. [30] It is known that PPZ, as a triazole compound, operates through a mechanism of action that involves the cell membrane. [10]

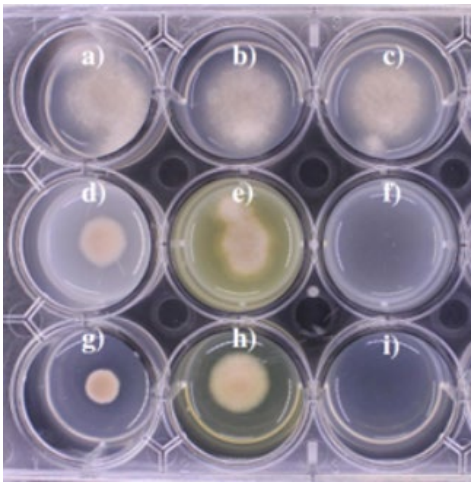

Fig. 2. Representative image of the 12 well plates used for the antifungal activity experiments: **(a)** Fungal growth control, **(b)** etOH, **(c)** PLA, **(d)** N-TA, **(e)** N-KE, **(f)** N-PPZ, **(g)** F-TA, **(h)** F-KE and **(i)** F-PPZ

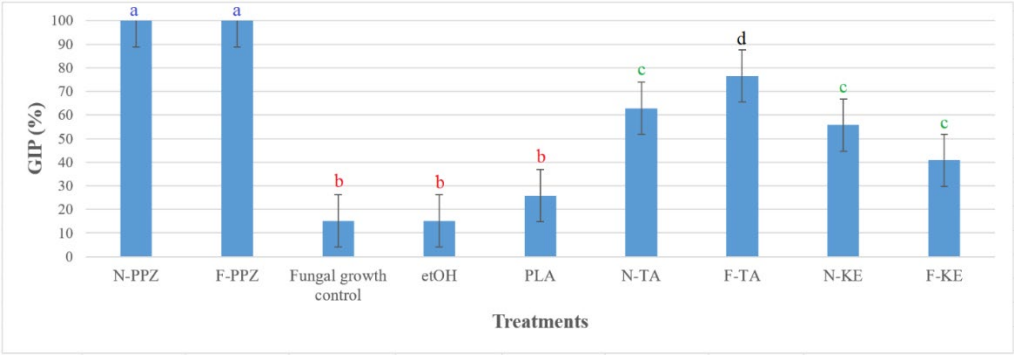

Fig. 3. Values of antifungal activity as a percentage of pathogen growth inhibition. Bars with the same letter do not differ significantly.

J. Mex. Chem. Soc. **2025**, *69*(3)
Regular Issue

ISSN-e 2594-0317

The antifungal activity experiments are illustrated in Fig. 3. The treatments of PPZ, both in their encapsulated and free forms, indicate complete inhibition of fungal growth. The etOH treatment shows no evidence of affecting fungal development, having no contribution to the antifungal activity when ethanol is used as vehicle for the AIs. The PLA treatment exhibit a 25 % inhibition in their composition, nevertheless, there is no significant statistical difference between this treatment and the growth inhibition perceived in the fungal growth control. In the case of F-TA, significantly higher inhibition is observed compared to its encapsulated form (N-TA), reaching nearly 80 %, while the nanoencapsulated form only reached close to 64 %. On the other hand, the KE treatments exhibited no significant statistical difference. Nanoencapsulation delays the release of fungicide molecules, reducing the amount of AI available to act on the fungus, thus reducing the growth inhibition obtained by using the free molecule. However, this condition did not affect the antifungal activity of KE due to the smaller size of the nanospheres obtained with this treatment.It has been reported that nanoparticles with sizes of several hundred nm enter cells through endocytosis, this mechanism being a disadvantage, since the nanoparticles often fail to escape the endocytic vesicles in which they are coated upon entering the cell. This leads to lower AI delivery efficiency. In contrast, smaller nanoparticles manage to permeate directly into the phospholipids of the cell wall without being trapped in vesicles, thus increasing their toxicity, this being a positive feature when the delivered molecule is a fungicide. [31] In the case of PPZ, its activity was not affected by nanoencapsulation due to the high antifungal activity of this molecule, achieving 100 % inhibition despite being slowly released. Due to low inhibition of fungal growth, compared to the other two molecules, ketone was eliminated from subsequent experiments.

Release profiles

The substance KE was excluded from the study due to its low solubility and antifungal activity, and was not considered in subsequent experiments. Fig. 4 shows the release profiles for the different treatments. It can be seen that, as they are nanoencapsulated, the fungicides have a slow release, which is desirable since the objective of this study is to reduce the amount of AI that could be in contact with the roots of the plant at a given time, thus reducing the risk of phytotoxicity.

The release of propiconazole for the F-PPZ and N-PP was completed at approximately 10 hr and 14 hr, respectively. The derivative compound (tertiary alcohol) in the N-TA treatment was fully released after 12 hr, while in the F-TA treatment, it nearly completed its release within 8 hr. The free form of the derivative released half of its content in the first hour, while in its encapsulated form, it experienced a delay in this process, whereas propiconazole exhibited a constant and progressive release with no significant variations over time. The initial burst release of F-PPZ occurred at 6.5 hr, while in N-PPZ, it reached an 80 % release at the 11th hour. Previous experiments with Barrera-Méndez et al. showed that propiconazole encapsulated in PLGA, a similar biocompatible polymer, had a 50 % release in 12 hours and finished dialyzing in 104 hours. [16] The encapsulated forms of each molecule exhibited a longer release profile due to the molecular diffusion that the AI has to endure by being entrapped in the PLA matrix. It is also worth notice that the FA releases a little faster than the PPZ in either their free of nanoecapsulated forms, respectively.

PLA has been found in previous research to have a sustained release pattern of up to 10 days as a nanocarrier, surpassing release limitations to extend its effectiveness over a longer period. The nanoparticles containing PLA and chitosan also showed evidence of sustained release of the active compound over a 2-week period in medical applications. [32] Furthermore, there is data from experiments where surfactants were added to PLA, and in these cases, it is observed that the complete drug release occurs within a time frame ranging from 6 to 12 days. [33]

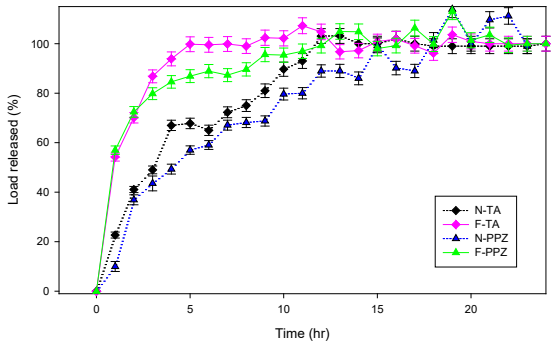

Fig. 4. Release profiles for the different treatments.

J. Mex. Chem. Soc. **2025**, *69*(3)
Regular Issue

ISSN-e 2594-0317

Phytotoxicity test

Fig. 5 illustrates the representative growth plates of an A. thaliana seedling with the most and least phytotoxic treatments (F-TA and N-TA, respectively) being compared to the negative control. The phytotoxicity impact of the treatments on the root length is shown in Fig. 6, while Fig. 7 shows the number of lateral roots obtained with each treatment. The PLA treatment shows no phytotoxic damage. The 5 % ethanol solution, used to dissolve the TA derivative, showed no evidence of damage to the primary roots, demonstrating no inhibition in the growth of the healthy seedling. The primary root, which was the main focus in previous studies by Bonilla et al., continues to demonstrate the highest inhibition and significant phytotoxicity in biological assays. [5]

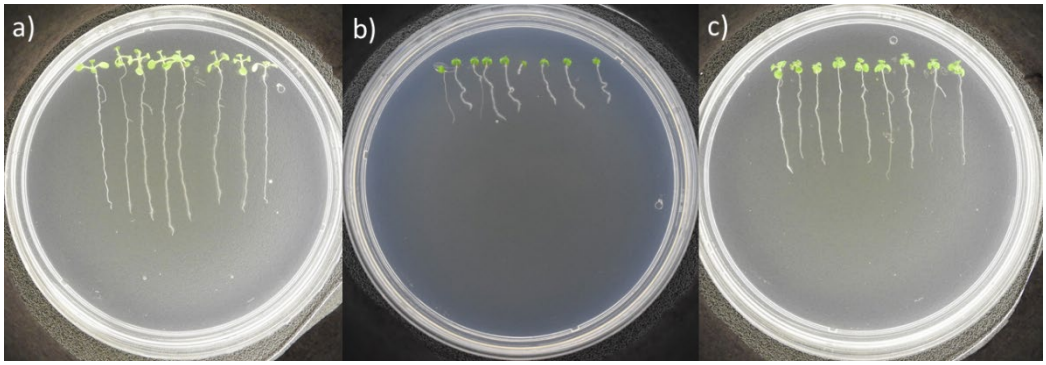

Fig. 5. Representative experiments of a Petri dish with developing *A. thaliana* seedling along with one of the treatments: **(a)** C-, **(b)** FTA, **(c)** N-TA.

The results revealed a significant difference between the N-TA treatment and the F-TA formulation, consistent with previous research conducted by Bonilla et al., where this molecule in its free form was identified as one of those with the most impact on the primary root. [5] The treatment of the derivative in its free form exhibit negative effects on root growth, resulting in a reduction of up to 60 % in the length of the primary root. On the other hand, when in its encapsulated form, the growth reduction was only of 35 %, showing less phytotoxic effects and indicating root protection for the seedling due to the slow release of the fungicide. This suggests that nanoencapsulation with the biodegradable polymeric matrix acts as a protective mechanism for plant roots, reducing the amount of fungicide in contact with the roots, since the AI molecule must first cross said matrix through molecular diffusion, which is a slow mechanism. In this way, the fungicide concentration is sufficient to control the fungal infection, but not so high as to damage the roots as much as the free molecule does.

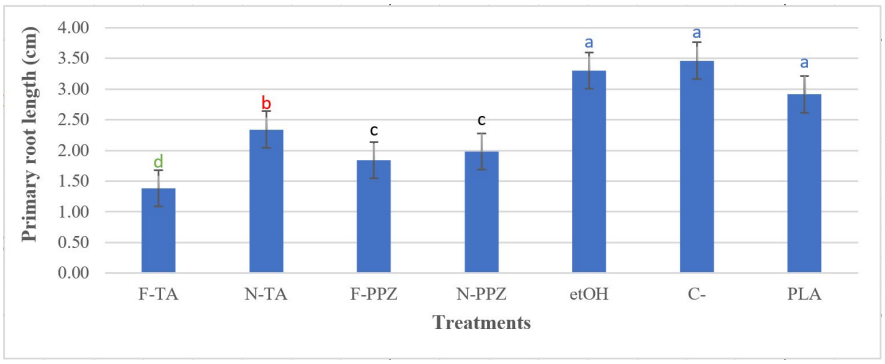

Fig. 6. Phytotoxicity analysis on primary root length. Bars with the same letter do not differ significantly.

J. Mex. Chem. Soc. **2025**, *69*(3)
Regular Issue

ISSN-e 2594-0317

The F-PPZ and N-PPZ formulations exhibit lower phytotoxicity compared to the derived molecule F-TA. The phytotoxicity levels of the treatments are consistent with the results obtained in the antifungal activity tests, being the treatments with the most biological activity also the most phytotoxic and viceversa. In the subsequent Fig.7, a summary of the analyses related to phytotoxicity in lateral roots is presented, as this parameter is considered an indicator of resistance and tolerance in drought situations. [34]

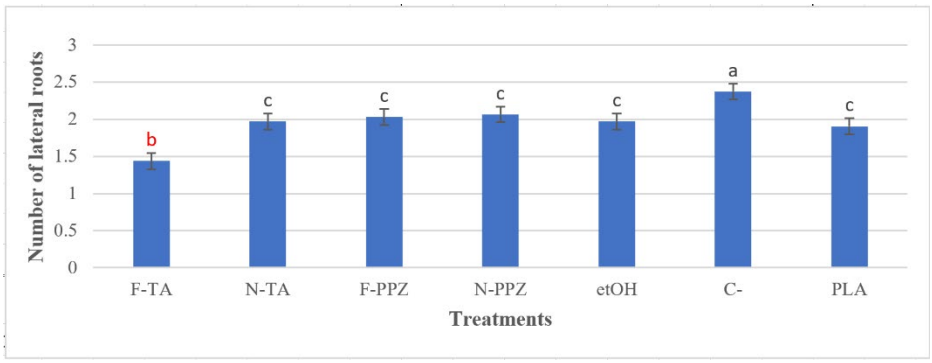

Fig. 7. Phytotoxicity analysis on lateral root. Bars with the same letter do not differ significantly.

The ethanol solution was introduced as a treatment to test its minimal involvement in seedling toxicity, primarily as a diluent for the TA molecule in the experiments. However, healthy seedlings show a slight variation in the number of lateral roots compared to this ethanol solution and empty nanoparticles with a polymer matrix. The TA molecule in its free form has the lowest number of lateral roots, but its nanoencapsulated formulation allows it to increase the number of lateral roots, demonstrating the protective action provided by nanoencapsulation attributed to the slow diffusion of the fungicide within the PLA matrix.

The length of the seedling's root appeared relatively favorable when compared to previous studies involving non-encapsulated molecules, as reported by Bonilla et al. [5] The same trend was observed in the analysis of lateral roots. This might suggest a potential protective effect of the active ingredient on the plant, as its free form exhibited greater toxicity. However, it is important to note that these parameters are not sufficient to be considered a comprehensive phytotoxicity analysis. To draw more robust conclusions, more advanced and costly methods or analyses, such as *in situ* tests and molecular investigations are needed to formalize and deepen the study.

Conclusions

The characterization of nanoparticles is essential for assessing their suitability as carriers for antifungal compounds. The results indicate that these particles have appropriate physicochemical properties, such as nanoscale size and high zeta potential, suggesting that they can remain stable in aqueous dispersions. Furthermore, the improvement in polydispersity with the addition of the PLA as a polymer matrix is a positive indicator of their quality and stability. Around 40 % of the active ingredient was successfully encapsulated within the formulations, with the highest yield achieved for the TA derivative formulation. This means that a significant amount of the compound can be released in a controlled and effective manner at the site of action. This can be especially useful in agricultural applications, where a gradual and sustained release of fungicides is required. It is important to note that, while there is a small reduction of about 15 % of the bioactivity of the TA molecule when nanoencapsulated, there is also an increase of near 70 % of the root length. The reduction of antifungal activity of the tertiary alcohol when nanoencapsulated happens because the molecule takes more time to take effect, since it must cross the polymeric matrix in which it is nanoencapsulated, as can be seen in its release profile. Although propiconazole must also pass through the PLA matrix, that molecule shows greater antifungal activity than the tertiary alcohol, so its bioactivity is not affected by its nanoencapsulation. In

J. Mex. Chem. Soc. **2025**, *69*(3)
Regular Issue

ISSN-e 2594-0317

contrast, this same delay in the release of the tertiary alcohol also reduced its phytotoxicity. These nanoencapsulated formulations demonstrate significant potential to enhance the effectiveness of fungicides while reducing phytotoxicity in plants. These findings could have practical applications in crop protection and sustainable agriculture. However, it is important to continue research and conduct long-term studies to evaluate their effectiveness under field conditions and their environmental impact.

Acknowledgments

This project was supported by the FORDECyT (Fondo Institucional de Fomento Regional para el Desarrollo Científico, Tecnológico y de Innovación, grant number 292399) from the Consejo Nacional de Humanidades, Ciencias y Tecnologías (CONAHCyT). The authors thank CONAHCyT for the Jahsive S. Quintero Beltrán Master's scholarship. Also, thanks to Laura Stefany Licona Velázquez for her support during the molecule synthesis and purification processes.

References

1. Tyśkiewicz, R.; Nowak, R.; Ozimek, E.; Jaroszuk-Ściseł, J. *Int. J. Mol. Sci.* **2022**, *23*, Article 4. DOI: https://doi.org/10.3390/ijms23042329.
2. Savary, S.; Ficke, S.; Aubertot, J.N.; Hollier, C. *Food Secur.* **2012,** *4*, 519-537. DOI: https://doi.org/10.1007/s12571-012-0200-5.
3. Gura, W.; Gelain, J.; Sikora, E.; Vinson, E.L.; Brannen, P.; Schnabel, G. *Plant Dis.* **2023**, Aug 14. DOI: https://doi.org/10.1094/PDIS-04-23-0778-RE.
4. Eatough Jones, M.; Kabashima, J.; Eskalen, A.; Mayorquin, J.; Carrillo, J.; Hanlon, C.; Paine, T. *J. Econ. Entomol.* **2017**, *110*, 1611-1618. DOI: https://doi.org/0.1093/jee/tox163.
5. Bonilla, I.; De La Cruz, O.L.; Sánchez, D.; Ortiz, R.; Rodríguez, B.; Barrera-Méndez, F.; Gómez, R.E.; Medrano, F.J.; Olivares, J.L. *J. Mex. Chem. Soc.* **2019**, *62*. DOI: https://doi.org/10.29356/jmcs.v62i3.531.
6. Bazzini, P.; Wermuth, C. Substituent Groups., in: *The Practice of Medicinal Chemistry: Fourth Edition* Georges, C.; Aldous, D.; Raboisson, P.; Rognan, D. Ed., Academic Press, London, **2008**, 319-357.
7. Baker, S.; Volova, T.; Prudnikova, S.V.; Satish, S.; Prasad, M.N. *Environ. Toxicol. Pharmacol.* **2017**, *53,* 10-17. DOI: https://doi.org/10.1016/j.etap.2017.04.012.
8. Arora, S.; Murmu, G.; Mukherjee, K.; Saha, S.; Maity, D. *J. Biotechnol.* **2022**, *355,* 21-41. DOI: https://doi.org/10.1016/j.jbiotec.2022.06.007.
9. Lopez, K.S., in: *Nanotransportadores de polifenoles: Aplicación en la industria cosmética [Polyphenol nanocarriers: application in the cosmetic industry]*. Disertation, University of Cartagena, Colombia. **2023.** DOI: https://doi.org/10.57799/11227/12239.
10. Shalini, K.; Kumar, N.; Drabu, S.; Sharma, P.K. *Beilstein J. Org. Chem.* **2011**, *7*, 668-677. DOI: https://doi.org/10.3762/bjoc.7.79.
11. Tan, D.; Yuan, P.; Annabi-Bergaya, F.; Dong, F.; Liu, D.; He, H. *Appl. Clay Sci.* **2015**, *114,* 190-196. DOI: https://doi.org/10.1016/j.clay.2015.05.024.
12. Abigail, E.A.; Samuel, M.; Chidambaram, R. *J. Taiwan Inst. Chem. Eng.* **2016**, *16,* 318-326. DOI: https://doi.org/10.1016/j.jtice.2016.03.024.
13. Viirlaid, E.; Riiberg, R.; Mäeorg, U. *Agronomy Research.* **2015**, *13*, 152–1159. DOI: https://doi.org/10.1016/j.jtice.2016.03.024.
14. Maruyama, C.R.; Guilger, M.; Pascoli, M.; Bileshy-José, N.; Abhilash, P.C.; Fraceto, L.F.; de Lima, R. *Sci. Rep.* **2016**, *6*, Article 1. DOI: https://doi.org/10.1038/srep19768.
15. Hwisa, N.; Katakam, P.; Rao, C.; Adiki, S. *VRI Biol. Med. Chem.* **2013**, *1*, 8-22. DOI: https://doi.org/10.14259/bmc.v1i1.29.

J. Mex. Chem. Soc. **2025**, *69*(3)
Regular Issue

ISSN-e 2594-0317

16. Barrera-Méndez, F.; Miranda, D.A.; Sánchez, D.; Bonilla, I.; Rodríguez, J.B.; Monribot, J.L.; Olivares, J.L. *J. Mex. Chem. Soc.* **2019**, *63*. DOI: https://doi.org/10.29356/jmcs.v63i1.564.
17. Öcal, H.; Arıca-Yegin, B.; Vural, İ.; Goracinova, K.; Çalış, S. *Drug Dev. Ind. Pharm.* **2014**, *40*, 560-567. DOI: https://doi.org/10.3109/03639045.2013.775581.
18. Ali, S.H.H.A.; Al-Qubaisi, M.; Hussein, M.Z.; Ismail, M.; Zainal, Z.; Hakim, M.N. *Int. J. Nanomedicine.* **2012**, *7,* 3351-3363. DOI: https://doi.org/10.2147/IJN.S30809.
19. Kuchovská, E.; Morin, B.; López-Cabeza, R.; Barré, M.; Gouffier, C.; Bláhová, L.; Cachot, J.; Bláha, L.; Gonzalez, P. *Sci. Total Environ.* **2021**, *764,* 142921. DOI: https://doi.org/10.1016/j.scitotenv.2020.142921.
20. Banpean, A.; Hararak, B.; Winotapun, C.; Wijaranakul, P.; Kitchaicharoenporn, S.; Naimlang, S. *J. Mater. Sci.* **2023**, *58*, 6823-6838. DOI: https://doi.org/10.1007/s10853-023-08418-2.
21. Xiao, R.Z.; Zeng, Z.W.; Zhou, G.L.; Wang, J.J.; Li, F.Z.; Wang, A.M. *Int. J. Nanomedicine* **2010**, *5,* 1057-1065. DOI: https://doi.org/10.2147/IJN.S14912.
22. Arpagaus, C. *J. Pharm. Investig.* **2019**, *49*, 405-426. DOI: https://doi.org/10.1007/s40005-019-00441-3.
23. Bohrey, S.; Chourasiya, V.; Pandey, A. *Nano Converg.* **2016**, *3*, 3. DOI: https://doi.org/10.1186/s40580-016-0061-2.
24. Hickey, J.W.; Santos, J.L.; Williford, J.M.; Mao, H.Q. *J. Control. Release.* **2015**, *219,* 536-547. DOI: https://doi.org/10.1016/j.jconrel.2015.10.006.
25. Wei, Q.; Wei, W.; Lai, B.; Wang, L.Y.; Wang, Y.X.; Su, Z.G.; Ma, G.H. *Int. J. Pharm.* **2008**, *359*, 294-297. DOI: https://doi.org/10.1016/j.ijpharm.2008.03.027.
26. Honary, S.; Zahir, F. *Trop. J. Pharm. Res.* **2013**, *12*, Article 2. DOI: https://doi.org/10.4314/tjpr.v12i2.19.
27. Zielińska, A.; Ferreira, N.R.; Feliczak-Guzik, A.; Nowak, I.; Souto, E.B. *Pharm. Dev. Technol.* **2020**, *25*, 832-844. DOI: https://doi.org/10.1080/10837450.2020.1744008.
28. Kamiya, H.; Gotoh, K.; Shimada, M.; Uchikoshi, T.; Otani, Y.; Fuji, M.; Matsusaka, S.; Matsuyama, T.; Tatami, J.; Higashitani, K., in: *Nanoparticle Technology Handbook,* Naito, M.; Yokoyama, T.; Hosokawa, K.; Nogi, K., Ed., Elsevier, London, UK, **2008**, 113–176.
29. Muzibur Rahman, M.; Mohamed Asiri, A., in: Advances in Colloid Science [Internet]. *IntechOpen* **2016.** DOI: https://doi.org/10.5772/62716, accessed in November **2023**
30. Yoshimi, A.; Miyazawa, K.; Abe, K. *J. Fungi* **2017**, *3*, Article 4. DOI: https://doi.org/10.3390/jof3040063.
31. Nakamura, H.; Watano, S. *ONA Powder Part. J.* **2018**, *35,* 49-65. DOI: https://doi.org/10.14356/kona.2018011.
32. Narayanan, V.H.; Kost, B.; Lewandowski, A.; Durai, R.D.; Wawrzyniak, P.; Biela, T.; Wingenfeld, R.; Sabeth, H.; Schwarzer, R.; Brzeziński, M. *Adv. Powder Technol.* **2023**, *34*, 104205. DOI: https://doi.org/10.1016/j.apt.2023.104205.
33. Mulia, K.; Geraldine, V.; Krisanti, E.A. *AIP Conf. Proc.* **2021**, *2344*, 040005. DOI: https://doi.org/10.1063/5.0047483.
34. Snapp, S.; Kirk, W.; Román-Avilés, B.; Kelly, J. *Hort. Science* **2003**, *38*, 187-191. DOI: https://doi.org/10.21273/HORTSCI.38.2.187.